Dimensions, Microstructure, Chemical, and Hygroscopic Analysis of Steam-Exploded Bamboo Fibers at Different Ages

Yanping Zou,[a,b,c] Wenjuan Zhao,[a,b,c] Wenfu Zhang,[a,c,]* Jian Zhang,[a,c] Ying Zhao,[a,c] Shaofei Yuan,[a,c] and Hong Chen [b]

Bamboo fibers (BFs) at different ages (1, 3, and 5 years old) were prepared by pretreatment and steam explosion. The results demonstrated that the separation degrees of BFs increased with the age of the bamboo. The combined effects of pretreatment and steam explosion partially removed the hemicellulose and lignin from BFs, while the crystalline structure of cellulose remained unaltered. The water vapor adsorption isotherms of BFs at different ages all showed a typical S-shape and could be classified as type II, and the hysteresis of BFs increased with the age of the bamboo. After pretreatment and steam explosion, the tissues in the vascular bundle were effectively crushed, and the parenchyma tissues were dislodged and separated from the fiber sheath. During the steam explosion process, hot steam penetrated the bamboo's pores, including the pores induced by pretreatment. This caused fractures and delamination in the interface between the vascular bundle and the parenchyma tissues. These cracks progressed layer by layer along the vascular bundle interface, leading to the fracture of the bamboo.

DOI: 10.15376/biores.19.1.1479-1493

Keywords: Bamboo fibers; Pretreatment; Steam explosion; Separation mechanism

*Contact information: a: Zhejiang Academy of Forestry, Hangzhou, Zhejiang, P.R. China, 310023; b: College of Furnishings and Industrial Design, Nanjing Forestry University, Nanjing, Jiangsu, P.R. China, 210037; c: Key Laboratory of Bamboo Research of Zhejiang Province, Hangzhou, Zhejiang, P.R. China, 310023; *Corresponding author: zhangwenfu542697@163.com*

INTRODUCTION

In recent years, there has been growing interest in natural fiber-based composites due to the increasing demand from consumers for lighter-weight, carbon-sequestering, and sustainable materials. This interest is also driven by ecological concerns, including environmental safety and recyclability. As a renewable resource, bamboo has numerous advantages such as wide distribution, abundant sources, and rapid growth. Consequently, it holds significant potential for applications in industries such as paper, biofuels, and textiles. The exceptional mechanical properties of bamboo primarily stem from its fiber components (Amada and Untao 2001; Lo *et al*. 2004). Bamboo fibers (BFs) offer several advantageous characteristics, including biodegradability, light weight, affordability, eco-friendliness, renewability, low energy extraction, and the ability to mitigate global warming. BFs find applications in various areas, including biofuel production, construction materials, paper and textile industries, the cosmetic industry, and the sports industry.

Bamboo is composed of structural fibers and matrix, which is made of parenchyma cells. Bamboo culm contains 50% parenchyma, 40% fibers, and 10% vascular bundles

(Alvin and Murphy 1988). The BFs form bundles that are bonded to each other in the longitudinal and lateral directions (Ray *et al*. 2005). Bamboo is composed of cellulose (45 to 55%), hemicellulose (15 to 25%), lignin (15 to 30%), pectin (0.5 to 1.5%), and other organic and inorganic compounds (Liu *et al.* 2011; Nayak and Mishra 2016; Rocky and Thompson 2018). Due to the high content of hemicellulose and lignin in natural bamboo, the degumming process is difficult, and the cellulose fibers cannot be separated easily. The extraction process and its subsequent manipulation are crucial in determining the properties and performance of BFs (Zakikhani *et al*. 2014). Adequate procedures can result in much better and easier extraction of fibers from the bamboo slivers, thereby minimizing fiber damage.

Different methods, including physical (Okubo *et al*. 2004), chemical, biological, and combined technologies, can be used to prepare BFs. Since the complex structure of bamboo and its high lignin content hinder fiber extraction in a timely manner, it is difficult to extract fibers using only one technology. Thus, combined technology, such as a combination of pretreatment of bamboo slivers using chemicals or enzymes and steam explosion, is commonly used to accelerate fiber production. Pretreatment, which is the most important and costly operation unit, is a prerequisite processing step in combined technology. Alkali treatment is a common pretreatment method. It can effectively delignify cellulose, chemically expand cellulose, enzymatically saccharify bamboo, and cut off the chemical connection between hemicellulose and lignin, removing most of lignin and hemicellulose (Yamashita *et al*. 2010; Kassaye *et al*. 2017). The steam explosion (SE) technique is a very common method to extract natural fibers in general. It has been known as an efficient way of separating lignin from woody materials utilized in the paper industry. SE includes an auto-hydrolysis step and an explosion step through the penetration of high-pressure steam into the plant cell wall. During the steam explosion, saturated steam penetrates the fibers. When the steam pressure is suddenly released, hemicellulose is hydrolyzed, and hemicellulose-lignin bonds are also cleaved, which increases the solubility of lignin in alkaline or organic solvents (Li *et al*. 2007). However, there has been little discussion about the damage mechanisms of pretreatment and steam explosion on BFs.

In this study, three kinds of bamboo at different ages are selected as raw materials for preparing BFs through pretreatment and steam explosion. The goal was to clarify the damage mechanism of pretreatment and steam explosion on BFs. The BFs were characterized by scanning electron microscopy (SEM), Fourier-transform infrared spectroscopy (FT-IR), X-ray diffraction (XRD), dynamic vapor sorption (DVS), thermogravimetric analysis (TGA), and micro-computed tomography (Micro-CT).

EXPERIMENTAL

Materials

Three different ages (1, 3, and 5 years old) of moso bamboo (*Phyllostachys pubescens*) were obtained from Zhejiang province, China. The bamboo culms at the height of 2 to 4 m from the base were cut. The bamboo culms were cut in the form of bamboo slivers with a length of 80 mm and a width of 15 mm. The sodium hydroxide (NaOH) was analytically pure and supplied by Chengdu Cologne Chemical Co., Ltd.

Chemical Pretreatment and Steam Explosion

Bamboo slivers were immersed in NaOH solution with a concentration of 5% at 100 ℃ for 1 h. Then, pretreated bamboo slivers were rolled and washed with water to remove the alkali. A certain quality of bamboo slivers and an equal quality of water were placed in the steam explosion device. The explosion pressure and explosion holding time were set to a certain value, and the heating device was powered on. The saturated steam produced was continuously fed into the explosion device to reach the preset experimental pressure, the valve was closed, and the timer was started. The BFs in the explosion chamber were sprayed into the receiving device when the set time was up, the BFs were collected and dried. The steam explosion and BF classification is shown in Fig. 1.

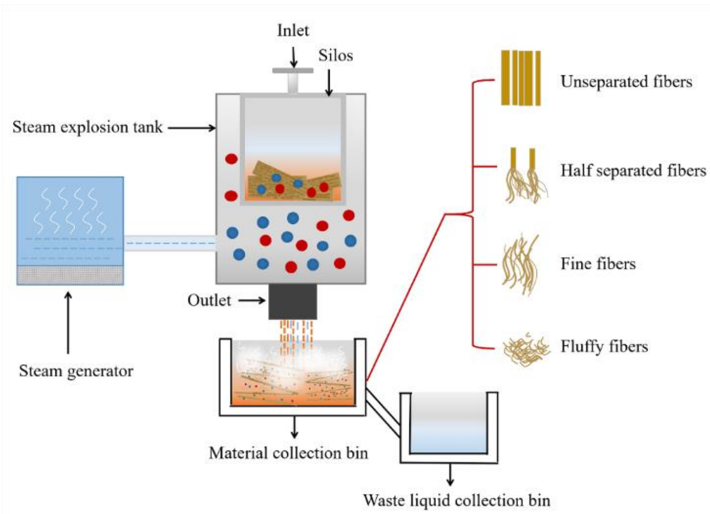

Fig. 1. Schematic of steam explosion and BF classification

A1, A3, and A5 are used here to represent BFs obtained from 1-year-old, 3-year-old, and 5-year-old bamboo, respectively. The fiber separation degree refers to the dispersion state of fibers, which is mainly related to their morphology. The BFs obtained from steam explosion were divided into four categories according to their morphology: fluffy fibers, fine fibers, half separated bamboo strips, and unseparated bamboo strips. Fluffy fibers are characterized by a flocculent appearance and the size is similar to bamboo powder. Fine fibers refer to fiber bundles less than 0.6 mm in diameter that have been fully separated. Half separated bamboo strips refer to materials where one end and the middle remain tightly connected while the other end is separated, and unseparated bamboo strips refer to wholly intact bamboo strips with no apparent separation.

Color Analysis

Color parameters were measured with a high-precision colorimeter (SR-68, KONICA MINOLTA, Japan) according to an international standard colorimetric system including the values L^*, a^*, and b^* (Chen *et al*. 2014). Three replicates were measured for each sample. The overall color difference (ΔE^*) was calculated according to Eq. 1,

$$\Delta E^* = [(\Delta L^*)^2+(\Delta a^*)^2+(\Delta b^*)^2]^{1/2} = [(L^*-L_0^*)^2+(a^*-a_0^*)^2+(b^*-b_0^*)^2]^{1/2} \quad (1)$$

where ΔE^* is the overall color difference, and L^*, a^*, b^* are the lightness, red-green feature and yellow-blue feature in the color, respectively. L_0^*, a_0^*, b_0^* are the data of the control group.

Microstructure and Chemical Composition Analysis

The sizes and morphology of BFs were measured by vernier caliper and a digital microscope (VHX-7000, KEYENCE, China). Thirty replicates were measured for each sample of the size test. The surface section and cross-section of the BFs were observed with a field emission scanning electron microscope (S-3400N, Hitachi, Japan). The FT-IR spectra of BFs were recorded with a spectrometer (VERTEX 80 V, Bruker, German) within the range of 4000 to 500 cm^{-1} at a resolution of 4 cm^{-1} and 64 scans. BFs were cut into powder for XRD testing. The crystal structure of cellulose in samples was measured using an X-ray diffractometer (XRD, Ultima IV, Rigaku, Japan) in a range of 2θ = 5 to 45° with a scanning rate of 10°/min with a CuKα radiation source. The crystalline index (*CrI*) of BFs was calculated by the commonly employed peak-height method (Segal *et al*. 1959), according to Eq. 2,

$$CrI = (I_{200} - I_{am})/I_{200} \quad (2)$$

where I_{200} is the intensity of the (200) peak at about 2θ = 22.4° after subtracting the background signal, and I_{am} represents the intensity of the amorphous region at about 2θ = 18°.

Thermogravimetric Analysis (TGA)

The thermal stability and degradation behavior of the BFs were examined with a thermogravimetric analyzer (TGA, STA409PC, Netzsch, Germany). The experiment was performed at a constant heating rate of 20 °C/min, from room temperature to 800 °C, under an inert atmosphere (pure nitrogen) with a flow rate of 20 and 40 mL/min.

Micro-computed Tomography (Micro-CT) Characterization

The microstructure of BFs at different ages was observed using micro-CT (Nano-Voxel 3000, China). Specifically, selected areas of half-separated fibers were scanned using a resolution of 5 µm. The micro-CT images of the cross-section of BFs were obtained to reveal the separating processes of BFs at different ages.

Dynamic Water Vapor Sorption

The moisture adsorption isotherms were measured using the DVS Resolution dynamic moisture adsorption instrument (Aquadyne DVS, Quantachrome, USA) in an atmosphere of high-purity nitrogen. The data curves were then analyzed to determine their moisture adsorption characteristics. To ensure consistency in the experimental conditions, the temperature was kept constant throughout the test. Samples weighing between 30 and 50 mg were placed in weighing bottles and dried thoroughly. In this study, the step mass change rate was set to be less than 0.001%/min, and the relative humidity range used was 0% to 95%. The humidity gradient was 0, 10, 20, 30, 40, 50, 60, 70, 80, 90, and 95%.

RESULTS AND DISCUSSION

Fiber Yield and Surface Morphology

The surface morphology of BFs at different ages is shown in Fig. 2a. The separation degrees of BFs were increased with the increase of bamboo age. The proportion of half-separated and unseparated fiber of A1 and A3 was much higher than A5, which was consistent with the results for the proportion of different types of BFs (Fig. 2b). A1 and A3 had tough surfaces with a lot of colloids and very few fiber separations. The separation of A5 was much higher than A1.

The proportion of different types of BFs at different ages is shown in Fig. 2b. The degree of dispersion and uniformity of BFs increased as the age of the bamboo increased. Although there was a slight difference in the ratio of fluffy fibers and fine fibers between A1 and A3, the ratio was significantly higher in A5 compared to A1 and A3. This difference in ratio may be attributed to the lignin content of bamboo, which increases with the age of the bamboo (Cheng *et al*. 2015; Zhu *et al.* 2020). In addition, the decrease in lignin content helps to reduce the occurrence of shear fractures caused by lignin degradation (Hao *et al*. 2018). Therefore, the lignin content was higher as the bamboo age increased, making it more prone to damage during the milling process, which facilitated steam penetration and resulted in more fine fibers.

Figure 2c shows the color parameters of the BFs at different ages. Δ*L** in A1 and A3 were similar and decreased abruptly in A5, which indicated that the lightness of BFs declined as bamboo ages increased. The Δ*E** values in A5 increased sharply compared to A1 and A3. The Δ*a** and Δ*b** values for BFs at different ages changed similarly which decreased slightly from A1 to A5. The color of BFs became a little reddish and greenish with the increase of bamboo ages.

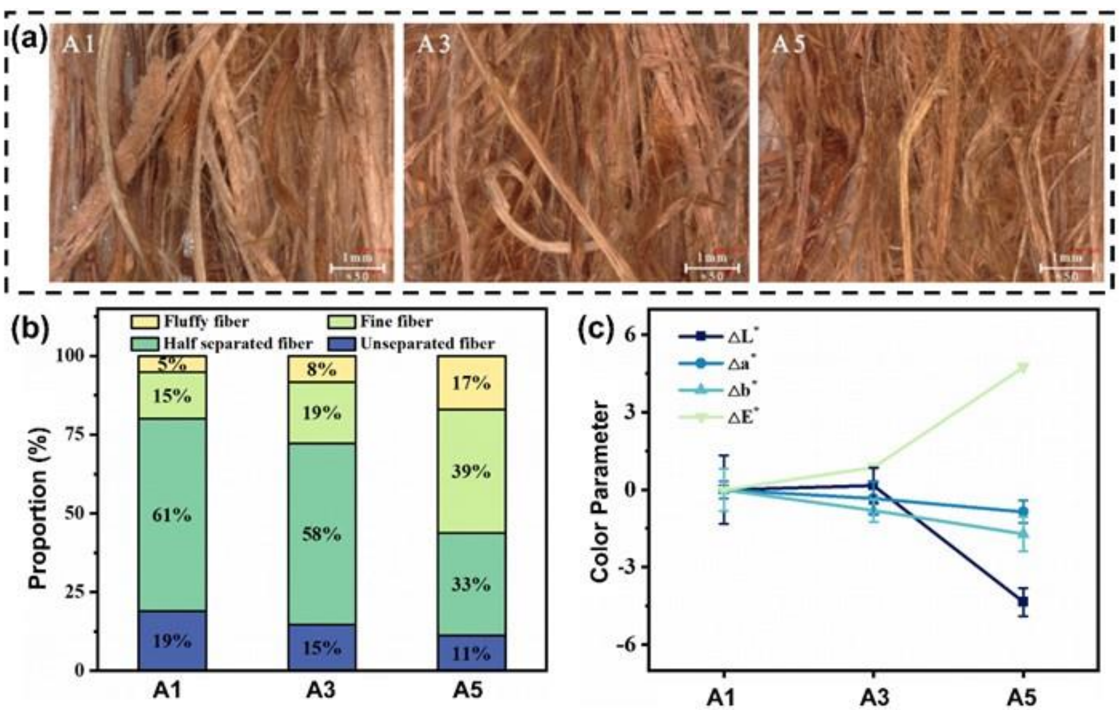

Fig. 2. a) Surface morphology, b) proportion of different types, and c) color parameters of BFs at different ages

Microstructure and Size

According to Fig. 3a, the surface of BFs was broken and many fragments appeared; the surface became rather rough and irregular, suggesting that those particles were lignin liberated from the cell wall by steam explosion treatment (Lu *et al*. 2020). The dispersion of BFs in the longitudinal sections of different ages was similar, and the fibers remained in bundles with no obvious tendency to separate. The cross-section of BFs at different ages is shown in Fig. 3b. Fiber bundles with intact and rigid structures were observed in A1, and the cross-sections of A3 and A5 began to separate, which demonstrated that alkali pretreatment and steam explosion removed most of the colloid. Fiber bundles were gradually cleaved and dissociated with the removal of hemicelluloses and lignin in A3 and A5. The separation of A5 was the highest; one can see from the cross-section of A5 that most of the fiber bundles were dispersed into single fibers. This is mainly because, under the action of high temperature and high-pressure water vapor, hemicellulose is partially hydrolyzed, whereas lignin is softened and easily degraded, thus reducing the strength of the connection between the fibers. The gas in the pores expands sharply, producing an explosion that splits the bamboo into fine fiber bundles, thus achieving the separation of components and structural changes of the raw material. This is the result of the combined effect of steam temperature and acetic acid produced by the degradation of hemicellulose.

The lengths and diameters of BFs at different bamboo ages are shown in Fig. 4. The average length and diameter of BFs increased and then decreased with the increasing age of bamboo. The increasing content of non-cellulose, the major component of the fibers, is responsible for the change in fiber diameter with age (Ebissa *et al.* 2022). The general trend for most of the processes was that the fineness decreased with the increase in length. This indicated that the longer the average length of the fibers, the less delignification occurred, and the number of fibers decreased along the length as the length increased. However, the fineness of the extracted fibers in this research is contrary. This is because the linear density of the extracted fibers can be proportional to the length of the respective fibers in the combined process when delignification is moderately applied in different stages of the process. Though BFs seem to be continuous in the bamboo culms between nodes, they are actually shorter in length when separated as individual fibers. This is due to bamboo cells in fibers overlapping with each other like flax fibers. Thus, fibers in bundle form had higher lengths and a higher linear density. Theoretically, fibers with shorter lengths had lower linear density and higher fiber fineness due to having fewer bundles and more individual fibers that were no longer attached to a longer bundle (Rocky and Thompson 2018).

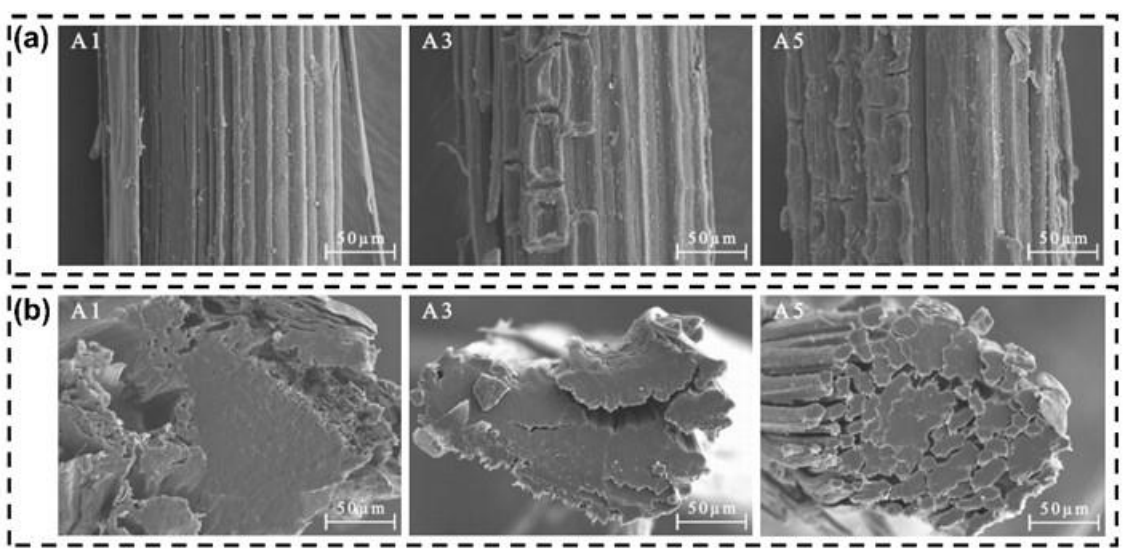

Fig. 3. The a) longitudinal section and b) cross-section of BFs at different ages

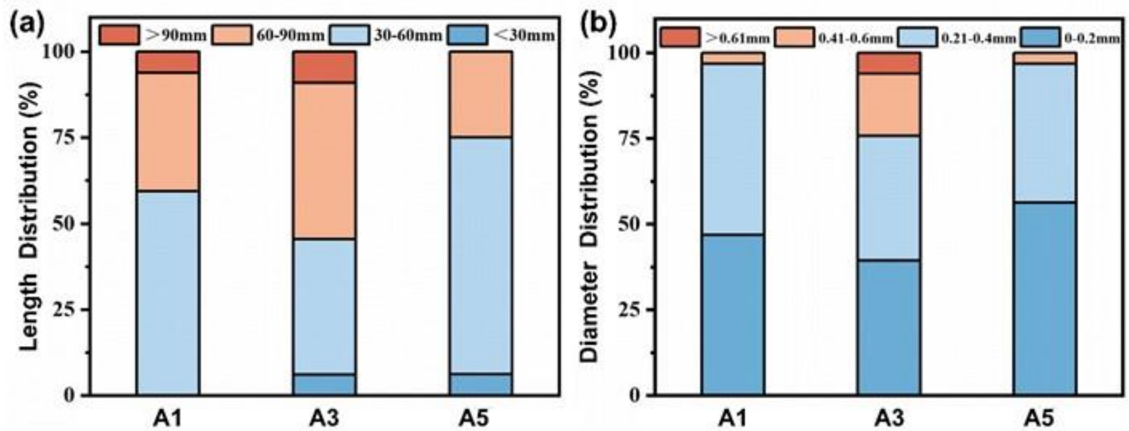

Fig. 4. The a) length distribution and b) diameter distribution of BFs at different ages

Table 1. Sizes of BFs at Different Ages

Samples	Average Length (mm)	Average Diameter (mm)
A1	59.12 (18.24)	0.22 (0.08)
A3	65.47 (21.96)	0.29 (0.18)
A5	55.30 (15.66)	0.21 (0.09)

Physicochemical Characteristics

As depicted in Fig. 5a, the results from all samples exhibited virtually comparable FTIR spectra. This demonstrated that no new functional groups were added to the cellulose molecules during the aging process from 1 year to 5 years (Morán *et al.* 2008; Cheng *et al.* 2015). The decrease in the intensity of the band at 1733 cm^{-1}, which is attributed to the C=O stretching vibration in xylan in hemicellulose and lignin of bamboo, confirmed the partial removal of hemicellulose and lignin in the BFs of different ages. The bands at 1509 and 1460 cm^{-1} were due to the aromatic skeleton vibration in lignin (Wang *et al*. 2020; Zhang *et al*. 2021). The intensity of the bands at 1509 and 1460 cm^{-1} were decreased in the A3 and A5 compared to A1, which indicated that the hemicellulose and lignin had been partly removed. The peak observed at around 1240 cm^{-1} was attributed to the acetyl group of lignin, and it became pronounced in A1. However, a decrement was observed in A3 and A5, further indicating that lignin had been removed. The absorption peaks of C-O-C at 1164 cm^{-1} and β-glycosidic linkage between the monosaccharides at 895 cm^{-1} came from cellulose. The intensity of the bands at 1164 and 895 cm^{-1} were decreased in the A3 compared to A1 and A5, which indicated that the cellulose had been degraded to a minor extent.

The XRD pattern of BFs at different ages is shown in Fig. 5b. The distinct peaks at 15.8°, 22.3°, and 34.7° corresponded to (1-10) and (110), (200), and (004) lattice planes, respectively (Nishiyama *et al.* 2002; Yang *et al.* 2017), which is characteristic for the typical cellulose I. The patterns of the fibers of different ages were the same as the cellulose I profile, suggesting that bamboo age did not affect cellulose crystalline structure in fibers. Figure 5c shows the *CrI* values of fibers; the crystallinity of A1, A3, and A5 was 69.64%, 67.88%, and 69.68%, respectively. The relative crystallinity of BFs decreased first and then increased with the increase in bamboo age, and the change in relative crystallinity of BFs at different ages may be caused by the difference in chemical composition in BFs.

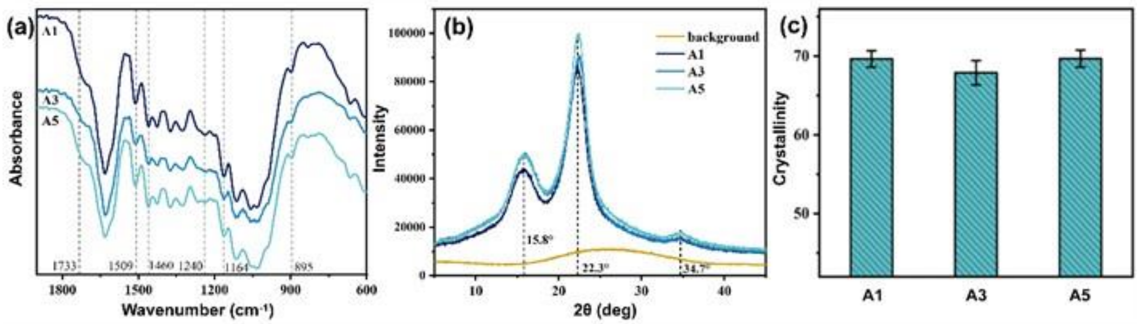

Fig. 5. a) FT-IR spectra, b) XRD pattern, and c) Crystallinity of BFs at different ages

The hygroscopicity of the material has a high correlation with the number of hygroscopicity groups in BFs. Among the main components of bamboo, hemicellulose has the most hygroscopic groups. The degradation of hemicellulose in fibers under the action of saturated steam will inevitably lead to the decrease of hydroxyl groups. On the other hand, the orientation of the cellulose amorphous zone in the fiber is improved after saturated steam treatment, and the hydroxyl groups between cellulose molecular chains will form hydrogen bonds, further reducing the number of hydroxyl groups available for other interactions, thereby reducing the moisture absorption of the process fiber. The age factor did not greatly affect the moisture content in bamboo.

The water vapor adsorption and desorption isotherms of the BFs at different ages are reported as the moisture content against relative humidity (RH), presented in Fig. 6. All of the isotherms exhibited a sigmoidal shape typical of bamboo and can be classified as type II according to the classification scheme (Brunauer *et al*. 1938). It was shown that in the lower relative humidity range, the isothermal adsorption process was dominated by the rapid water adsorption of the monolayer on the hydroxyl adsorption site (Hill *et al*. 2010). However, in the relatively low humidity range, the growth rate of water adsorption of fast monolayer was low. The growth rate of the equilibrium moisture content of the fibers was significantly larger when RH was relatively high, especially above 70%. This was due to the softening of the fibers at high relative humidity, which led to the expansion of the cell wall matrix and the formation of more water absorption sites, resulting in an increase in the equilibrium water content, whereas desorption isotherms were more linear at similar RH levels.

There was no significant difference in the water content of BFs at different ages, but there was a slight difference in the degree of hysteresis. As shown in Fig. 7a, BFs exhibited the hysteresis phenomenon over the entire RH region, but the degree of hysteresis varied. Hysteresis for BFs at different ages increased first and then decreased with increasing RH, but the highest hysteresis values varied from 3.13 to 3.45% at 70% RH, and the hysteresis of A3 and A5 was slightly higher than A1, which indicated that bamboo age had a certain effect on hysteresis. The variation in the change in the hysteresis coefficient was remarkable (range 0.42 to 0.91) for BFs at different ages. The hysteresis coefficient increased with increasing RH when RH was between 10 and 70% (Fig. 7b). When RH > 70%, the moisture content in the cell wall was close to saturation, and the hysteresis coefficient increased linearly with the increase of RH, which conforms to the general characteristics of biomass materials. At room temperature, softening of hemicellulose occurs around 75% RH. The viscosity and rigidity of the polymer network structure formed by the crosslinking of hemicellulose and lignin will decrease, and the capacity of the cell wall to contain water molecules will increase. In order to inhibit the expansion of the cell wall and prevent water molecules from entering the cell wall, lignin, which plays a role in strengthening the cell wall, will also increase the hygroscopic hysteresis. The one-year-old culms had lower holocellulose and Klason lignin contents than the three- and five-year-old culms, which were similar (Li *et al*. 2007); this may be the reason why A3 and A5 had higher hysteresis than A1.

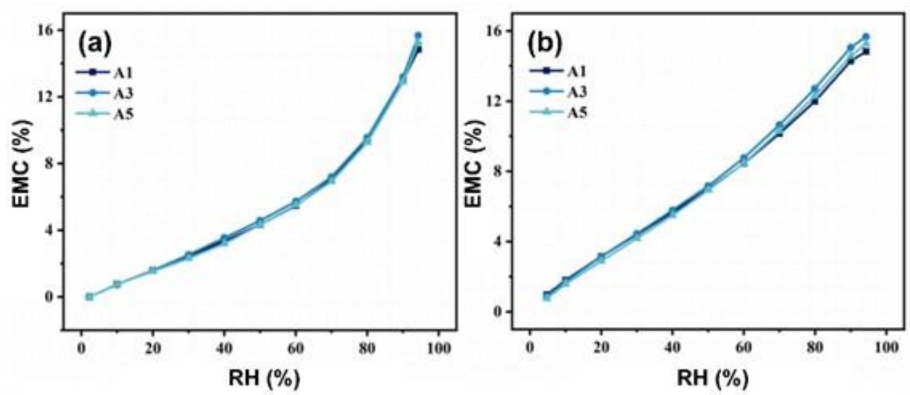

Fig. 6. EMC values of BFs at different ages plotted against RH during a) adsorption and b) desorption

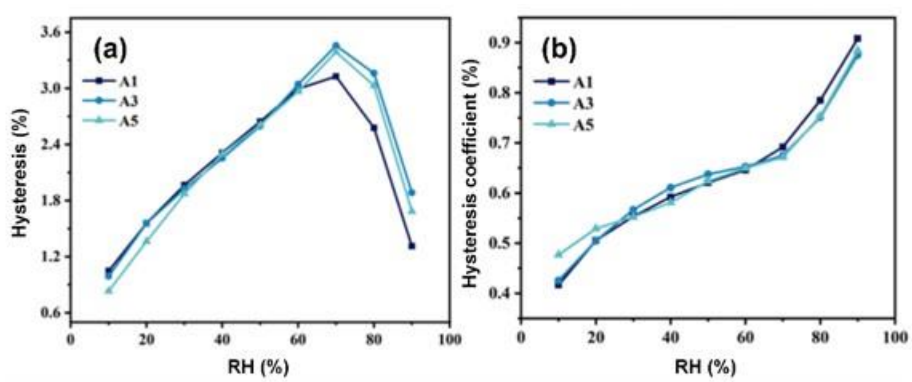

Fig. 7. a) Hysteresis and b) hysteresis coefficient of BFs at different ages

Thermal Properties

Typical TGA and DTG curves of the BFs at different ages are shown in Fig. 8. Three distinct weight loss stages in the BFs at 30 to 120 °C, 200 to 380 °C, and 380 to 420 °C, respectively. The first stage of degradation is the dehydration phase. This phase has been attributed to moisture and some extractive evaporation in the fiber (Hernandez-Mena *et al.* 2014). Next zone degradation is known as active pyrolysis where the rate of mass loss is rapid corresponding to the decomposition of hemicellulose, cellulose, and lignin. In the first degradation stage, the mass losses that began in BFs of different ages were negligible between temperatures of 116 to 216 °C. The TGA curve displayed the decomposition of hemicellulose followed by the breakdown of cellulose at this stage (Zakikhani *et al.* 2015). A3 at first degradation showed a mass loss of about 5.95%; therefore, A3 degraded more hemicellulose than A1 and A5. From Table 2, BFs degraded cellulose at high temperatures in the range of 216 to 273 °C. The degradation of cellulose takes place at higher temperatures due to its crystalline structure and will cause higher stability compared to hemicellulose. Following the degradation of cellulose, the degradation of lignin takes place in the range 273 to 405 °C. Lignin is a component that contains an aromatic compound unlike hemicellulose and cellulose, which is the main component of the cell wall (Peng *et al.* 2012). It has a complex structure, which involves bonding the hemicellulose and cellulose together. Therefore, the decomposition of lignin is slow and more difficult during the entire temperature (Alwani *et al.* 2013). The higher mass loss in the third stage of decomposition will cause less thermal stability due to more lignin degradation. As can be seen in Table 2, the main composition removal of the fibers caused the weight loss in the first, second, and third degradation stages. The T_{max} refers to the decomposition temperature corresponding to the maximum weight loss. With increasing bamboo age, there was a slight increase in the T_{max} of BFs. Additionally, the TGA and DTG curves of BFs at different ages exhibited a high degree of overlap, suggesting that the age variations of 1, 3, and 5 years did not significantly impact the properties of the fibers.

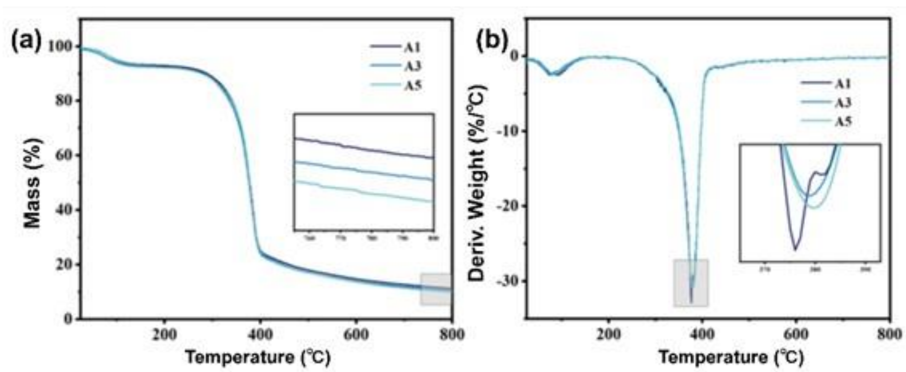

Fig. 8. Typical a) TGA curves and b) DTG curves of BFs at different ages

Table 2. Thermogravimetric Data of BFs at Different Ages

Samples	Dehydration	Active Pyrolysis			Passive Pyrolysis
	Weight loss (%) at 25 to 100 °C	1st degradation: weight loss (%) at 116 to 216 °C	2nd degradation: weight loss (%) at 216 to 273 °C	3rd degradation: weight loss (%) at 273 to 405 °C	Char residue (%) at 800 °C
A1	5.11	1.34	1.59	66.81	11.19
A3	5.95	1.23	1.58	67.25	10.51
A5	5.19	1.70	1.75	66.48	9.86

The Separation Mechanism

The separating behavior of half-separated BFs at different ages was further scanned by micro-CT to investigate its separation mechanisms. During the steam explosion process, hemicellulose and lignin produced some acidic substances, which degraded hemicellulose into soluble sugar, and the lignin was softened and partially degraded in the composite intercellular layer, thus weakening the adhesion between fibers. High-pressure hot steam enters the fiber raw material and penetrates the internal fiber voids, and when the pressure is released instantaneously, the hot steam molecules that have penetrated the fiber interior are released instantaneously at high speed from the relatively closed voids in the form of airflow, causing a certain degree of mechanical fracture of the fiber (Jacquet *et al.* 2015). As shown in Fig. 9, under the combined effect of alkali treatment and steam explosion, firstly the damage occurred at the weak lap point of ground tissue, where the micro cracks generated, developed, and diffused. Because of the weaker interface between vascular bundles and ground tissue, it broke into the interface and the delamination cracking occurred and began delamination extension to both sides along the interface of vascular bundle when the crack tip developed to the vascular bundles. There was a redistribution of internal stress when the vascular bundles were suddenly broken, transferring the load on the vascular bundles rapidly to the surrounding ground tissues. The strength of the ground tissues was far lower than that of the vascular bundles, so instantly the ground tissues suffered a brittle fracture. The new generated crack continued to extend forward, leading to the damage of the next vascular bundle and eventually resulting in the failure of the whole bamboo. The organization in the vascular bundles was basically crushed. The parenchyma material was shed and separated from the fibrous sheath. A series of irregular cracks were produced in the fiber sheath, which divided it into several fiber bundles at different sizes.

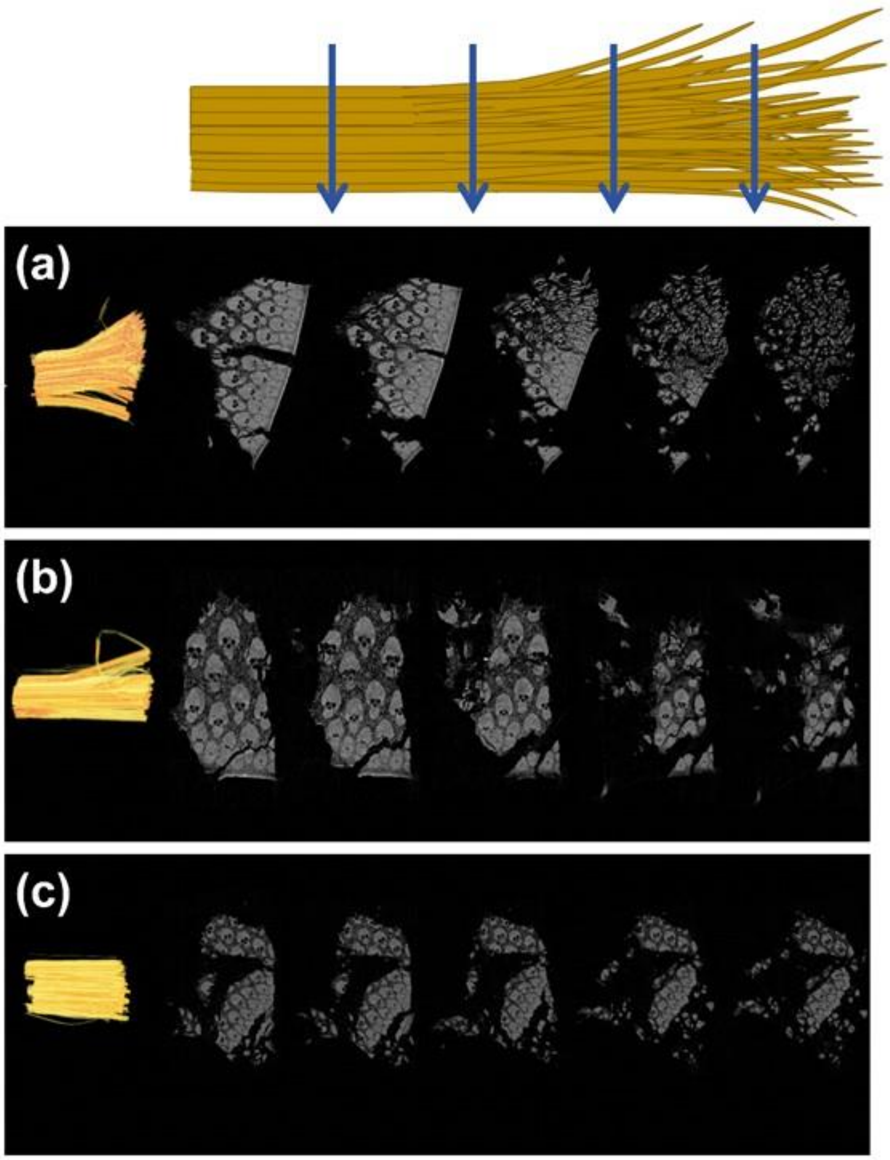

Fig. 9. The micro-CT images of half-separated BFs at different ages. a) 1-year-old BFs, b) 3-year-old BFs, and c) 5-year-old BFs

The one- and three-year-old fibers showed a distinct separation at one end and a tight connection at the other. The five-year-old fibers showed a uniform separation from end to end. This indicated that the steam could penetrate deeper into the five-year-old bamboo during the explosion process to separate the fibers, while the one-year and three-year bamboo hindered the penetration of steam, resulting in a large difference in the separation of the two ends of the fibers. This phenomenon was mainly related to the effect of bamboo rolling. During the pre-treatment process of bamboo, rolling was carried out to increase the specific surface area and enhance the explosion effect (Zhao *et al*. 2023). Bamboo with higher stiffness is more easily rolled open, resulting in more cracks and increasing the pathway for steam penetration, thereby achieving a more uniform separation. The stiffness of bamboo is related to its chemical composition and varies with bamboo age (Huang *et al*. 2012). The lignin content of one to six-year-old bamboo shows an increasing trend (26 to 36%), while the relative content of cellulose decreases (55 to 45%), and the content of hemicellulose remains stable (Zhu *et al.* 2020). Lignin is an important chemical constituent of bamboo because it holds the fibers together and provides stiffness to bamboo (Jain and Kumar 1994). Previous studies have shown that five-year-old moso bamboo has the highest mechanical properties and hardness compared to one- and three-year-old bamboo (Han *et al.* 2023). Therefore, five-year-old bamboo is more prone to being rolled open, thus creating excessive vapor infiltration paths, which improves the uniformity of separation and results in the highest yield of fine fibers.

CONCLUSIONS

1. The separation degrees of bamboo fibers (BFs) were increased with the increase of bamboo age. The proportion of fine fiber of A5 was 39%. Big bundles were gradually cleaved and dissociated with the removal of consisted of hemicelluloses and lignin.
2. Under the combination of pretreatment and steam explosion, the hemicellulose and lignin in BFs were partially removed, and the removal effect of hemicellulose and lignin was better with the increase of bamboo age. The bamboo age did not affect cellulose crystalline structure in fibers.
3. The water vapor adsorption isotherms of BFs at different ages all showed a typical S-shape and can be classified as type II. The hysteresis of BFs of different ages increased first and then decreased, and the hysteresis of A3 and A5 was slightly higher than that of A1, which indicated that the hysteresis of BFs increased with the age of bamboo.
4. During the steam explosion process, hot steam enters the pores of the bamboo and the pores produced by pretreatment, the interface between the vascular bundle and the parenchyma tissues fractures and delamination cracks that ultimately lead to the separation of BFs. The older the bamboo, the better the rolling effect. The increase in surface area indicates that there were more steam penetration paths generated, which is conducive to the entry of steam and achieving uniform steam explosion, thereby improving the yield of fine fibers.

ACKNOWLEDGMENTS

This research was supported by the National Key R&D Program of China No. 2023YFD2202100, the "Pioneer" and "Leading Goose" R&D·Program of Zhejiang (No. 2022C04019)

REFERENCES CITED

Alvin, K. L., and Murphy, R. J. (1988). "Variation in fibre and parenchyma wall thickness in culms of the bamboo *Sinobambusa tootsik*," *IAWA J* 9(4), 353-361. DOI: 10.1163/22941932-90001095

Alwani, M. S., Khalil, H. P. S. A., Sulaiman, O., Islam, M. N., and Dungani, R. (2013). "An approach to using agricultural waste fibres in biocomposites application: Thermogravimetric analysis and activation energy study," *BioResources* 9(1), 218-230. DOI: 10.15376/biores.9.1.218-230

Amada, S., and Untao, S. (2001). "Fracture properties of bamboo," *Compos. B. Eng.* 32, 451-459. DOI: 10.1016/S1359-8368(01)00022-1

Brunauer, S., Emmett, P. H., and Teller, E. (1938). "Adsorption of gases in multimolecular layers," *J. Am. Chem. Soc.* 60(2), 309-319. DOI: 10.1021/ja01269a023

Chen, Y., Tshabalala, M. A., Gao, J., Stark, N. M., and Fan, Y. (2014). "Color and surface chemistry changes of extracted wood flour after heating at 120 °C," *Wood Sci. Technol.* 48, 137-150. DOI: 10.1007/s00226-013-0582-3

Cheng, L., Adhikari, S., Wang, Z., and Ding, Y. (2015). "Characterization of bamboo species at different ages and bio-oil production," *J. Anal. Appl. Pyrolysis* 116, 215-222. DOI: 10.1016/j.jaap.2015.09.008

Ebissa, D. T., Tesfaye, T., Worku, D., and Wood, D. (2022). "Characterization and optimization of the properties of untreated high land bamboo fibres," *Heliyon* 8, e09856. DOI: 10.1016/j.heliyon.2022.e09856

Hao, H., Tam, L. H., Lu, Y., and Lau, D. (2018). "An atomistic study on the mechanical behavior of bamboo cell wall constituents," *Compos. B. Eng.* 151, 222-231. DOI: 10.1016/j.compositesb.2018.05.046

Hernandez-Mena, L. E., Pécoraa, A. A., and Beraldob, A. L. (2014). "Slow pyrolysis of bamboo biomass: analysis of biochar properties," *Chem. Eng. Trans.* 37, 115-120. DOI: 10.3303/CET1437020

Hill, C. A. S., Norton, A., and Newman, G. (2010). "Analysis of the water vapour sorption behaviour of Sitka spruce [*Picea sitchensis* (Bongard) Carr.] based on the parallel exponential kinetics model," *Holzforschung* 64, 469-473. DOI: 10.1515/hf.2010.059

Huang, Y. H., Fei, B. H., Yu, Y., and Zhao, R. J. (2012). "Plant age effect on mechanical properties of moso bamboo (*Phyllostachys heterocycla* var. *pubescens*) single fibers," *Wood Fiber Sci* 44(2), 196-201.

Jacquet, N., Maniet, G., Vanderghem, C., Delvigne, F., and Richel, A. (2015). "Application of steam explosion as pretreatment on lignocellulosic material: A review," *Ind. Eng. Chem. Res.* 54(10), 2593-2598. DOI: 10.1021/ie503151g

Jain, S., and Kumar, R. (1994). "Processing of bamboo fiber reinforced plastic composites," *Mater Manuf Process* 9(5), 813-828. DOI: 10.1080/10426919408934955

Kassaye, S., Pant, K. K., and Jain, S. (2017). "Hydrolysis of cellulosic bamboo biomass into reducing sugars via a combined alkaline solution and ionic liquid pretreatment steps," *Renew. Energ.* 104, 177-184. DOI: 10.1016/j.renene.2016.12.033

Li, X., Tabil, L. G., and Panigrahi, S. (2007). "Chemical treatments of natural fiber for use in natural fiber-reinforced composites: A review," *J Polym Environ* 15, 25-33. DOI: 10.1007/s10924-006-0042-3

Liu, L., Wang, Q., Cheng, L., Qian, J., and Yu, J. (2011). "Modification of natural BFs for textile applications," *Fibers Polym* 12, 95-103. DOI: 10.1007/s12221-011-0095-3

Lo, T. Y., Cui, H. Z., and Leung, H. C. (2004). "The effect of fiber density on strength capacity of bamboo," *Mater. Lett.* 58, 2595-2598. DOI: 10.1016/j.matlet.2004.03.029

Lu, H., Lin, X., He, B., and Zhao, L. (2020). "Enhanced separation of cellulose from bamboo with a combined process of steam explosion pretreatment and alkaline-oxidative cooking," *Nord Pulp Paper Res* 35, 386-399. DOI: 10.1515/npprj-2020-0007

Morán, J. I., Alvarez, V. A., Cyras, V. P., and Vázquez, A. (2008). "Extraction of cellulose and preparation of nanocellulose from sisal fibers," *Cellulose* 15, 149-159. DOI: 10.1007/s10570-007-9145-9

Nayak, L., and Mishra, S. P. (2016). "Prospect of bamboo as a renewable textile fiber, historical overview, labeling, controversies and regulation," *Fash Text* 3, 2. DOI: 10.1186/s40691-015-0054-5

Nishiyama, Y., Langan, P., Chanzy, H. (2002). "Crystal structure and hydrogen-bonding system in cellulose Iβ from synchrotron X-ray and neutron fiber diffraction," *J. Am. Chem. Soc.* 124, 9074-9082. DOI: 10.1021/ja0257319

Okubo, K., Fujii, T., and Yamamoto, Y. (2004). "Development of bamboo-based polymer composites and their mechanical properties," *Compos. Part A Appl. Sci. Manuf.* 35, 377-383. DOI: 10.1016/j.compositesa.2003.09.017

Peng, P., Peng, F., Bian, J., Xu, F., and Sun, R. C. (2012). "A comparative study of bamboo (*Phyllostachys incarnata* Wen) milled wood lignin and the successively alkali-fractionated lignins," *Wood Sci Technol* 46, 871-885. DOI: 10.1007/s00226-011-0451-x

Ray, A. K., Mondal, S., Das, S. K., and Ramachandrarao, P. (2005). "Bamboo—A functionally graded composite-correlation between microstructure and mechanical strength," *J Mater Sci* 40, 5249-5253. DOI: 10.1007/s10853-005-4419-9

Rocky, B. P., and Thompson, A. J. (2018). "Production of natural BFs-1: Experimental approaches to different processes and analyses," *J. Text. Inst.* 109, 1381-1391. DOI: 10.1080/00405000.2018.1482639

Segal, L., Creely, J. J., Martin Jr., A. E., and Conrad, C. M. (1959). "An empirical method for estimating the degree of crystallinity of native cellulose using the X-ray diffractometer," *Text. Res. J.* 29, 786-794. DOI: 10.1177/004051755902901003

Wang, Q., Wu, X., Yuan, C., Lou, Z., and Li, Y. (2020). "Effect of saturated steam heat treatment on physical and chemical properties of bamboo," *Molecules* 25, article 1999. DOI: 10.3390/molecules25081999

Yamashita, Y., Shono, M., Sasaki, C., and Nakamura, Y. (2010). "Alkaline peroxide pretreatment for efficient enzymatic saccharification of bamboo," *Carbohydr. Polym.* 79, 914-920. DOI: 10.1016/j.carbpol.2009.10.017

Yang, X., Shang, L., Liu, X., Yang, S., and Tian, G. (2017). "Changes in bamboo fiber subjected to different chemical treatments and freeze-drying as measured by nanoindentation," *J .Wood Sci.* 63, 24-30. DOI: 10.1007/s10086-016-1590-3

Zakikhani, P., Zahari, R., Sultan, M. T. H., and Majid, D. L. (2014). "Bamboo fibre extraction and its reinforced polymer composite material," *Int. J. Chem. Biomol. Metall. Mater. Sci. Eng.* 8(4), 271-274. DOI: 10.5281/zenodo.1092110

Zakikhani, P., Zahari, R., Hameed Sultan, M. T., and Abang Abdul Majid, D. L. (2015). "Thermal degradation of four bamboo species," *BioResources* 11, 414-425. DOI: 10.15376/biores.11.1.414-425

Zhang, Y., Yu, Y., Lu, Y., Yu, W., and Wang, S. (2021). "Effects of heat treatment on surface physicochemical properties and sorption behavior of bamboo (*Phyllostachys edulis*)," *Constr Build Mater.* 282, 122683. DOI: 10.1016/j.conbuildmat.2021.122683

Zhao, W., Zhang, J., Zhang, W., Yuan, S., Chen, H., and Wu, A. (2023). "Effect of bamboo unit morphology on the preparation of bamboo fibers by steam explosion," *Ind Crops Prod* 202, article 117066. DOI: 10.1016/j.indcrop.2023.117066

Zhu, Y., Huang, J., Wang, K., Wang, B., Sun, S., Lin, X., Song, L., Wu, A., and Li, H. (2020). "Characterization of lignin structures in *Phyllostachys edulis* (Moso bamboo) at different ages," *Polymers* 12(1), 187. DOI: 10.3390/polym12010187

Article submitted: October 24, 2023; Peer review completed: December 9, 2023; Revised version received: December 22, 2023; Accepted: January 1, 2024; Published: January 12, 2024.

DOI: 10.15376/biores.19.1.1479-1493